Title

Enhanced Innate Antiviral Gene Expression, IFN-α, and Cytolytic Responses Are Predictive of Mucosal Immune Recovery during Simian Immunodeficiency Virus Infection

Journal

The Journal of Immunology, 192(7)

ISSN

0022-1767

Authors

Verhoeven, David
George, Michael D
Hu, William
et al.

Publication Date

2014-04-01

DOI

10.4049/jimmunol.1302415

Peer reviewed

Published in final edited form as:
J Immunol. 2014 April 1; 192(7): 3308–3318. doi:10.4049/jimmunol.1302415.

Enhanced innate anti-viral gene expression, interferon-α, and cytolytic responses are predictive of mucosal immune recovery during SIV infection

David Verhoeven, **Michael D. George**, **Will Hu**, **Angeline T. Dang**, **Zeljka Smit-McBride**, **Elizabeth Reay**, **Monica Macal**, **Anne Fenton**, **Sumathi Sankaran-Walters**, and **Satya Dandekar**
Department of Medical Microbiology & Immunology, University of California, Davis, CA 95616

Abstract

The mucosa that lines the respiratory and gastrointestinal (GI) tracts is an important portal of entry for pathogens and provides the first line of innate immune defense against infections. Although an abundance of memory CD4+ T-cells at mucosal sites render them highly susceptible to HIV infection, the gut and not the lung experiences severe and sustained CD4+ T-cell depletion and tissue disruption. We hypothesized that distinct immune responses in the lung and gut during the primary and chronic stages of viral infection contribute to these differences. Using the simian immunodeficiency virus (SIV) model of AIDS, we performed a comparative analysis of the molecular and cellular characteristics of host responses in the gut and lung. Our findings showed that both mucosal compartments harbor similar percentages of memory CD4+ T-cells and displayed comparable cytokine (IL-2, IFN-γ, and TNFα) responses to mitogenic stimulations prior to infection. However, despite similar viral replication and CD4+ T-cell depletion during primary SIV infection, CD4+ T-cell restoration kinetics in the lung and gut diverged during acute viral infection. The CD4+ T-cells rebounded or were preserved in the lung mucosa during chronic viral infection that correlated with heightened induction of type I interferon (IFN) signaling molecules and innate viral restriction factors. In contrast, the lack of CD4+ T-cell restoration in the gut was associated with dampened immune responses and diminished expression of viral restriction factors. Thus, unique immune mechanisms contribute to the differential response and protection of pulmonary versus GI mucosa and can be leveraged to enhance mucosal recovery.

Keywords

mucosa associated lymphoid tissue; T-cell homeostasis; memory T-cell; type I interferon; simian immunodeficiency virus; viral restriction factor

INTRODUCTION

The mucosal immune system in the gastrointestinal (GI) and respiratory tract provides an effective barrier to the environment that is well programmed for generating rapid innate

Corresponding Author: Satya Dandekar, Ph.D. Dept. of Medical Microbiology and Immunology GBSF, Room 5511, University of California Davis, California 95616. Tel. 530 752-3409 Fax: 530 754-7240 sdandekar@ucdavis.edu.

immune response against pathogenic organisms (1, 2). However, in HIV infected patients, an increased incidence of gastrointestinal and pulmonary infections reflects a life-threatening disruption of mucosal barrier functions. An abundance of memory CCR5+ CD4+ T-cells in the gut and lung mucosa sets the stage for pathogenesis by providing an abundance of highly susceptible HIV targets. (3). Robust viral replication and severe CD4+ T-cell depletion has been shown to occur in the GI tract very early during HIV infection of humans and simian immunodeficiency virus (SIV) infection of rhesus macaques (3-9). While severe CD4+ T-cell depletion in the gut mucosa persists through all stages of HIV and SIV infections, the lung mucosa has been shown to preserve a high proportion of the memory CD4+ T-cells during chronic viral infection stage (10). However, the differences in the antiviral response between the GI and lung mucosa that may contribute to better CD4+ T-cell preservation and/or restoration in the lung during HIV/SIV infection remain poorly understood.

Although investigations of innate antiviral responses in the GI and lung mucosa to HIV infection have been understandably limited, some insights have been gained through investigations of pathogenic SIV infection in rhesus macaques. Recent studies in the SIV model showed that several IFN-α responsive cytokines are rapidly induced in lymphoid but not oral and GI mucosal tissues in response to pathogenic SIV infection (11). Additional SIV studies indicate that IFN-α induction and activation of tyrosine kinase 2 and STAT1 is suppressed in the central nervous system, but appears to be activated in the lung (12). Collectively, these findings suggest that the lung mucosa may employ a distinct set of antiviral mechanisms that provide an immunological advantage over mechanisms available in other mucosal compartments.

Importantly, IFN-α is associated with control over viremia during the acute stages of viral infection and can restrict viral replication in permissive cells (13). However, IFN-α-induced cytokine responses in the chronic SIV infection are associated with the severity of viral infection and strong IFN-α induction that may drive poor virological outcomes. In the African Green Monkey (AGM) model of non-pathogenic SIV infection, IFN-α and its responsive cytokines are rapidly induced during primary acute infection but are down-regulated during the chronic stage of infection (14). In contrast, IFN-α and its response-associated cytokines remain elevated in rhesus macaques with chronic SIV infection and are correlated with progression to simian AIDS (SAIDS). An induction of IFN-α expression in the chronic infection with other persistent viruses is also associated with incomplete control of viral replication and persistent but limited antiviral responses (15, 16). Therefore, we sought to determine the mucosal compartmental changes associated with SIV infection in rhesus macaques with respect to IFN-α signaling and the divergent mucosal responses, control of viral burden, and CD4 T-cell rebound in the context of innate signaling. A better understanding of the innate and adaptive immune host responses in each mucosal compartment that can restore CD4 T-cells could elucidate therapeutic targets to limit SIV pathogenesis.

In the present study, we utilized the SIV model to gain insights into the mechanisms of divergent innate antiviral responses between the lung and GI compartments and to investigate any potential immunological advantage they impart for immune recovery. We

performed a comprehensive molecular and cellular analysis of immune responses in the jejunum, colon, and lung of rhesus macaques during primary and chronic stages of SIV infection. Our findings suggest that the GI and lung mucosa diverge in the magnitude of CD4+ T-cell loss, despite having comparable levels of resident memory CD4+ T-cell percentages prior to SIV infection, and similar levels of viral replication during primary viral infection. Genes encoding type I IFN signaling molecules and viral restriction factors were induced at higher levels in the lung compared to the GI mucosa, and CD8+ T-cells from the lung showed an increased capacity for poly-functional SIV antigen-specific responses. Our findings suggest that robust induction and dominance of innate antiviral mechanisms in the lung mucosa compared to the gut mucosa may lead to a rebound and increased survival of CD4+ T-cells, thereby maintaining an effective adaptive immune response and limiting pathogenesis within this compartment.

MATERIALS AND METHODS

Ethics statement

Non-human primate studies were performed according to the recommended guidelines of (USDA) as well as the UC Davis IACUC (Approval# 05-11822 and 8472). Animals were housed at the California National Primate Research Center (CNPRC) and monitored for signs of illness. Housing and care of the animals including social (continuous pairing), cage (chew toys, coconuts), and food (fruits, vegetable and foraging mixtures) enrichment were conducted as per guidelines with no exceptions. Animals were anesthetized with ketamine and atropine and maintained on isofluorane for peripheral blood and tissue sample collection. Respiratory rate, blood pressure and response to stimulus of the animals were monitored during sample collection. Post-operative animals were treated with enrofloxacin and metronidazole. At the end of the study, animals were euthanized by ketamine anesthesia followed by barbiturate overdose. Animals were euthanized prior to the development of simian AIDS disease.

Animals and viral infection

Ten healthy colony-bred male rhesus macaques (Chinese/Indian hybrids) from the CNPRC were intravenously infected with 100 animal infectious doses of SIVmac251 (n=10). Five animals underwent longitudinal lung bronchio-alveolar lavage (BAL) washes while ten animals were subjected to upper GI endoscopy for obtaining longitudinal jejunal biopsy samples. SIV infected animals were necropsied at 8-10 weeks (n=5) and at 30 weeks post-infection (n=5). SIV-negative healthy macaques served as negative controls (n=5).

Cell isolation and flow cytometry

Lungs were perfused with sterile saline prior to sample collection. Jejunum, lung, and colon tissues were collected in RPMI and digested twice in 1mg/ml Collagenase IV (Sigma, St Louis MO) at 37°C for 45 minutes. Dissociated lymphocytes were purified on a Ficoll gradient (Atlanta Biologicals) and strained through 40μM cell strainers into RPMI-10. Non-specific binding was blocked by reacting the cells with 1% human gamma globulin (Sigma) in FACS staining buffer. The 13-parameter multicolor flow cytometry was performed using a modified LSR II (BD, San Jose CA) utilizing live gating with amine reactive dyes

(Invitrogen) and doublet discrimination. Antibodies (BD, San Jose CA and eBioscience, San Diego CA) for CD3 APCCy7 (SP34.2), CD4 Pacific Blue (OKT4), CD8 APCCy5.5 (3B5), Ki67 FITC (Ki-S5), CCR7 biotin (MAB179A) and QDot 605 streptavidin, CD25 PE (M-A251), CD2 PECy5.5 (S5.5), CD95 PECy5 (DX2), CD27 APC (O323), CXCR4 APC (12G5), CD28 Alexa 488 (CD28.2), CD62L FITC (SK11), CD45RA Pacific Blue or FITC (Mem-56), CD20 PECy7 (2H7), CD69 PECy7 (FN50), CCR5 PE (3A9) were used. Cell permeabilization for Ki67 detection was performed using 2X Fix/Perm (BD) and 0.01% Triton X-100 in staining buffer. Data were analyzed by FlowJo software (Treestar, Ashland OR).

SIV-specific T-cell responses

Virus-specific CD8+ T-cell responses in peripheral blood or mucosal lymphocytes were measured using overlapping SIV gag mac251 peptides (NIH, AIDS Reagents) in an 11-parameter 3 cytokine flow cytometric assay as previously described (17). Antibodies for IL-2 FITC (MQ1-17H12), Interferon-γ PECy7 (B27), and TNF-α PE (MabB11) were used (BD Biosciences). Gating for the cytokine-positive cells was set using media only controls and the positive threshold response was set by SEB controls with live gating using violet amine dye (Invitrogen) and doublet discrimination. Perforin PE (Pf-80/164) and CD107a APC (eBioH4A3) were stained directly ex vivo. Data were evaluated using SPICE program (Mario Roederer, VRC, NIAID, NIH).

Viral loads

SIV RNA loads in plasma and tissue samples were determined by real-time polymerase chain reaction (RT-PCR) assay as previously described (17-19).

Immunohistochemistry

Five micron thick OCT embedded tissue sections were blocked with 10% Goat serum and 1% Fc Blocker (Miltenyi Biotec) for 1 hour. Antibodies for CD3 (Dako, Capenteria CA), Ham56 (Dako), and p27 (NIH AIDS Reagents) were diluted at 1:100, 1:100, and 1:25 respectively in TBS with 0.05% Triton X-100 and incubated overnight at 4°C. Tissue sections were washed in TBS with Triton X-100 followed by anti-rabbit Cy3, anti-mouse IgM Cy5, and anti-mouse IgG Alexa 488 (Jackson ImmunoResearch, TX) and mounted using SlowFade with DAPI (Invitrogen, Carlsbad CA). Images were acquired using LSM 5 confocal microscope with PASCAL software using Cy5 and Alexa 488 on the first pass and DAPI and Cy3 on the second pass (Zeiss, Germany).

Macrophages were identified by immunostaining acetone-fixed cryopreserved tissue sections with anti-HAM56 antibody (DAKO). Briefly, tissue sections were blocked with 3% hydrogen peroxide for 30 minutes prior to antibody incubation at 1:100 for one hour at room temperature and washed in PBS, stained and visualized using the LSAB II peroxidase kit (DAKO). Tissue sections were counterstained with methyl green or hematoxylin and mounted with Permount. Macrophage numbers were quantified by counting immunostained cells in 15 tissue sections with similar architecture from uninfected and SIV-infected animals and averaged to get a total macrophage count per mm^2 of tissue for each animal.

RNA extraction and transcriptome analysis

Total RNA was extracted (RNeasy RNA isolation kit, Qiagen, Valencia, CA) and mRNA amplification, labeling, hybridization to rhesus macaque whole genome GeneChips©, (Affymetrix, Santa Clara, CA) staining, and scanning were performed (Affymetrix Gene Expression Analysis Technical Manual) at the host microbe and systems biology core at the University of California, School of Medicine as described previously (5, 20).

Analysis of Affymetrix GeneChip© data was performed using Robust Multi-array Analysis (RMA) algorithms (GeneSpring©, v9). Starting with the probe-level data from the arrays, the perfect-match (PM) values were background-corrected using a kernel density estimation and Fast Fourier Transformation. All the arrays were subsequently normalized together using quantile normalization, ensuring equal distribution of expression values across experimental groups (uninfected and SIV infected) and mucosal compartments (lung, colon, jejunum). The log-transformed expression values were then summarized using median polishing and following a linear additive model.

A minimum fold-change of 50% (p-value ≤ 0.05) was used as cut off criteria for identifying differentially expressed genes between uninfected healthy controls and SIV infected animals. Genes meeting fold-change and statistical criteria were then functionally categorized and the pathways and processes statistically enriched in the data were identified with Ingenuity Pathway Analysis software. The entire microarray data set is deposited at the Gene Expression Omnibus in the National Center for Biotechnology (https://www.ncbi.nlm.nih.gov/geo/query/acc.cgi?acc=GSE51615).

Gene expression levels of BST2, MX-1, and Viperin in mucosal tissues were measured by real time PCR assays (Taqman, Applied Biosystems, CA) utilizing previously published protocols (17). Values were normalized to the house-keeping gene GAPDH and calibrated to the corresponding tissue of uninfected animals. Final gene expression values were calculated using the $\Delta\Delta C_T$ method (21).

Statistical analysis

Statistical analysis was performed using the program Minitab (State College, PA) and GraphPad Prism version 5.00 for Windows (GraphPad Software, San Diego CA). The significance of the difference of viral loads, cell proliferation, CD4+ T-cell percentages, NK cells, and CD8+ T-cell percentages between pulmonary and gut mucosal sites were determined using ANOVA and Student T tests and p-values <0.05 were considered significant.

RESULTS

Gastrointestinal and pulmonary mucosal compartments are enriched with memory CD4+ T-cells that express HIV co-receptors

To determine the baseline levels of T-cell subsets in the lung, colon, and jejunum, we measured percentages of CD4+ and CD8+ T-cells, and quantified CD4+ T-cell effector memory (22) and central memory (T_{CM}) subsets in each compartment in healthy animals.

Each mucosal site harbored comparable percentages of CD4+ and CD8+ T-cells (Figure 1A). However, the jejunum had higher percentages of $CD4^{+high}CD8^{+low}$ double positive cells (4.8-6.5% of CD4+ T-cells), while double positive T-cells in the lung and colon were primarily $CD4^{+low}CD8^{+high}$ (14-28% and 10-15% of total CD8+ T-cells respectively) (Figure 1B). Most of the T-cells were $CD95^{high}$ (Figure 1E) and expressed CD69 (cell activation marker), indicating that each mucosal compartment harbored T-cell subsets with activated memory phenotype (Figure 1E). Notably, the majority of CD4+ T-cells in the GI and lung mucosa also expressed HIV coreceptors CCR5 (33-51% in each compartment) or both CCR5 and CXCR4 (49-68% in each compartment), (Figure 1D).

Central memory phenotypes (CCR7+) comprised 50-68% of all CD4+ T-cells in the jejunum and colon (Figure 1C). This population was also CD27+ and CD28+ (data not shown). However, high CCR5 expression on these cells may indicate that a large proportion of these cells might have been transitioning from central memory to effector memory pools (17). Fewer central memory CD4+ T-cells (2-11.5%) were detected in the lung.

The healthy baseline functional characteristics of mucosal T-cells are likely to influence their response to viral infection and thereby impact early viral replication kinetics (23). To determine whether T-cell functional characteristics are divergent between the GI and pulmonary compartments in healthy animals, we compared cytokine expression profiles of mucosal CD4+ T-cells following mitogenic stimulations with *Staphylococcus* enterotoxin B (SEB). Our findings suggest that the percentage of memory CD4+ T-cells that secreted interleukin-2 (IL-2), interferon-γ (IFN-γ) or polyfunctional (IL-2/IFN-γ) were comparable across all mucosal compartments (3.3-5.45%) (Figure 1F). In summary, both the GI and pulmonary mucosa of healthy macaques appear to be enriched with memory CD4+ T-cells that have comparable levels of HIV co-receptor expression and display similar levels of mitogen-activated cytokine production.

Altered transcriptional profiles of the GI and lung mucosa in SIV infected animals compared to SIV-negative healthy controls

We sought to determine whether lung and gastrointestinal mucosa of healthy animals displayed inherent baseline physiological differences that could impact their response to SIV infection or influence pathologic outcomes. To obtain a comprehensive molecular profile, we performed high throughput gene expression analyses utilizing rhesus macaque specific DNA microarrays. Changes in the gene expression of the lung, colon and jejunum from SIV infected animals were compared to baseline levels in uninfected animals and were subjected to non-biased hierarchical clustering to identify divergent transcriptional profiles for downstream biofunctional analysis (Figure 2A). The number of genes modulated during chronic SIV infection was notably higher in the lung (586) than in the colon (121) or jejunum (142). In addition, the jejunal mucosa appeared to display the greatest animal-to-animal variability. Interestingly, we also discovered that, in healthy uninfected animals, genes associated with type I interferon responses (RIG I, IFNAR2, STAT1, ADAR, MX2 and OAS3) were, in general, expressed at higher levels in the lung compared to the GI mucosa (Figure 2B), suggesting that the lung could be more efficiently “primed” for a rapid response to viral pathogens. In addition, expression of toll-like receptors (TLR) 1, 2, 4, 5,

and 8 was also elevated in the lung compared to the GI tract (Figure 2C). The expression of multiple TLRs at higher baseline levels in the mucosal tissues indicates that the lung may also have an inherent kinetic advantage over the GI tract in sensing and responding to infectious microbes through pathogen-associated molecular patterns (PAMPS).

Distinct chemokine expression profiles were observed in the colon and jejunum (elevated CCL15 and CXCL14) compared to lung (elevated CCL18 and CXCL17), suggestive of preferential recruitment of specific T-cell subsets to these sites (Figure 2D). Increased expression of CCL15 and CXCL14 suggests that the intestinal mucosa might recruit higher proportions of monocytes than the lung of healthy animals (24, 25). In contrast, expression of CCL18 in the lung may be indicative of increased numbers of naive T-cells being recruited into the regulatory T-cell pool (26). Collectively, the divergence in transcriptional profiles of healthy GI and lung mucosa appear to reflect the unique immunological microenvironment of each compartment, dictated by the cellular composition and the antigenic milieu that is normally encountered. Importantly, these profiles represent distinct physiological signatures that can be utilized to evaluate the effects of SIV infection in each mucosal compartment individually and in comparison to other mucosal compartments.

Comparable levels of SIV replication in gastrointestinal and respiratory mucosa

To compare the magnitude of viral replication in the lung and GI mucosal compartments, we measured levels of SIV RNA by real-time PCR. Viral loads at 2 weeks or 8-10 weeks post-SIV infection were not significantly different among mucosal sites (10^4 to 10^6 viral RNA copies/ml plasma) (Figure 3A). Viral replication persisted in each compartment during chronic stage of SIV infection (30 weeks post-infection). These data are intriguing since jejunum, despite the severe CD4+ T-cell depletion, did not have significantly different viral loads compared to the lung or colon, suggesting that other cell types may play a role in maintaining high levels of viral replication in the GI mucosa. It is also possible that viral transcripts were expressed at a higher level in the infected cells.

To characterize mucosal cell targets of SIV that may contribute to viral burden, we examined for the presence and co-localization of SIV p27 with either CD3 (T-cell marker) or Ham56 (macrophage marker) by immunohistochemistry at 30 weeks post-infection. Numerous SIV p27-posiitve macrophages were detected in lung, colon and jejunum mucosal tissues (Figure 3B). SIV-positive macrophages in the lung were scattered throughout the alveolar spaces as well as in interstitial tissues. SIV-infected macrophages in the colon and jejunum were localized both in lamina propria and near the crypt regions of the villi. To quantify the contribution of infiltrating macrophages to SIV infection in each mucosal site, we measured the influx of macrophages (Ham56+) in tissues from SIV infected animals and compared them to the baseline numbers present in SIV-negative control tissues (Figure 3C-D). The infiltration of macrophages was, in general, uniform among mucosal sites with slightly higher numbers observed in the colon. Our findings are in agreement with previous studies of the SIV model (27, 28), and suggest that mucosal compartments throughout the body may be highly permissive to infiltration by virally infected monocytes/macrophages as well as CD4+ T-cells.

The CD4+ T-cells are restored/preserved in the lung, but not in the GI mucosa during chronic SIV infection

To gain insights into potential divergence in the SIV mediated CD4+ T-cell depletion between the GI and lung mucosal compartments, we compared CD4+ T-cell levels in the lung, colon, and jejunum tissues after 1-2 weeks, 8-10 weeks, and at 30 weeks of SIV infection. During early acute infection (<4 wks post-infection), CD4+ T-cells were depleted to less than 5% of the total T-cell population in bronchoalveolar lavage (BAL) that was followed by a substantial rebound of CD4+ T-cell numbers (Figure 4A). In contrast to lung mucosa, jejunal mucosa showed severe depletion of CD4+ T-cells at one week post-SIV infection that persisted throughout the acute stage (Figure 4B). Our findings regarding the depletion of CD4+ T-cells in BAL are similar to those previously reported in SIV infected macaques with rapid disease progression and in HIV infected patients (29, 30).

During early and late chronic SIV infection (>8 wks), severe CD4+ T-cell depletion persisted in jejunal mucosa (Figure 4C). At 30 weeks post-infection, the jejunum (1-8% CD4+ T-cells of total CD3+ T-cells versus 60% in uninfected animals) had the lowest percentages of CD4+ T-cells as compared to the colon (8-13%) or lung mucosa (14-20%). Our findings suggest that mechanisms protecting CD4+ T-cells from severe depletion may have been more effective in lung mucosa than the jejunal and colonic mucosal sites (10, 31). Of note, CD4+ T-cells in peripheral blood (data not shown) were 32-45% of the total CD3+ T-cell pool, of which 30-39% were of memory phenotype (CD95+CD45RA-) suggesting that severe CD4+ T-cell depletion was occurring mainly in the mucosa during primary acute and early chronic stages of infection.

CD4+ T-cell restoration/retention in the lung mucosa is associated with enhanced innate antiviral gene expression

To determine whether efficient CD4+ T-cell restoration/retention in the lung during chronic SIV infection was associated with induction of host defense response mechanisms and specific molecular networks that were distinct from those in the GI tract, we evaluated the transcriptional profiles of lung compared to those of colon, and jejunum (Fig. 2A). While there was some overlap observed in the gene expression among mucosal compartments in response to SIV infection, about twice as many genes were transcriptionally modulated in the lung than in the jejunum and about 4-5 times as many as in the colon (Figure 5). In general, the physiological processes enriched in each mucosal compartment during chronic SIV infection were highly divergent and distinct from each other. A marked increase of gene expression was seen in the lung involving genes that mediate innate antiviral immunity as well as adaptive immune responses, while minimal changes were detected in the expression in these functional gene categories in intestinal mucosal compartments.

Upon closer examination, we found that the expression of molecules involved in type I interferon (IFN) production, signaling, and response were induced at significantly higher levels in the lung than in the intestinal mucosa (Figure 6A). Production of type I IFN might have been induced through RIG-I stimulation, and signaling through STAT-1 and STAT-2, which appeared to be linked to downstream expression of effector molecules such as OAS-1 and MX-1. Indeed, several well-established viral restriction factors induced by type I IFN

were up regulated at higher levels in the lung than in the GI tract, including tetherin, APOBEC3B, TRIM5, viperin, SAMHDI, and theta defensin-1 (Figure 6B).

To evaluate whether differences in innate antiviral response between the lung and the GI tract emerged in chronic SIV infection or were established earlier in the course of SIV infection, we measured and compared the magnitude of induction of viral restriction factors BST2/tetherin, MX-1, and Viperin in each compartment by quantitative real-time PCR (RT-PCR). At 2 weeks post-infection, we found that expression of tetherin MX-1 and viperin significantly increased over uninfected controls, but did not increase similarly in the jejunum or colon (Figure 7). Moreover, we determined that the coefficients of determination were strong between the level (%) of intestinal CD4 T-cells and expression levels of MX-1 (0.77) or viperin (0.86) transcripts of the animals during the chronic stage of SIV infection (data not shown). These data validated findings of the transcriptome analysis using DNA microarrays during chronic SIV infection, and indicate that the enhanced induction of antiviral mechanisms in the lung compared to the GI tract occurred early during the acute stage of infection and diverged thereafter.

Differential virus-specific CD8+ T-cell cytolytic functions in the lung and GI tract

We reasoned that restoration of CD4+ T-cells in the lung might have contributed to the helper functions that might have led to more effective cytolytic anti-viral CD8+ T-cell responses in the pulmonary mucosal compartment. Therefore, we performed immunophenotypic analysis by flow cytometry and gene expression profiling by DNA microarrays to evaluate cytolytic potential in all 3 mucosal compartments. A comparison of the levels of degranulating (CD107a+) versus perforin+ CD8+ T-cells indicated that ~39% of CD8+ T-cells in the lung of healthy uninfected macaques expressed intracellular perforin (Figure 8A). In contrast to the lung, few perforin+ CD8+ T-cells were detected in the colon and jejunum of SIV-negative animals. SIV infection led to an increased number of perforin+ CD8+ T-cells in each compartment. However, perforin+ CD8+ T-cells comprised only 17% and 18% (mean values) of the total CD8+ T-cell population (15-20%) in the GI compartments as compared to a mean of 41% in the lung (35-55%).

Despite the presence of higher numbers of perforin+ CD8+ T-cells in the lung during SIV infection, the functional efficacy of those CD8+ T-cells has not been well investigated. We therefore examined the ability of CD8+ T-cells from each mucosal compartment to produce multiple cytokines in response to stimulation with SIV antigens. Notably, the highest percentage of SIV antigen specific poly-functional CD8+ T-cells expressing both IL-2 and IFN-γ was detected in the lung (Figure 8B). These data are in agreement with previous studies of HIV infected patients (10), and highlight the importance of mucosal CD8+ T-cell responses in the control of viral replication. In support of the increased functional efficacy of T-cells, transcriptional profiling showed higher levels of granzymes K and H in the lung mucosa than in the gut mucosa (Figure 8C). Collectively, these data suggest that increased functionality of SIV-specific CD8+ T-cell responses in the lung mucosa may be inextricably linked to better CD4+ T-cell restoration and T-cell helper functions following resolution of primary acute stage of infection.

Discussion

The host encounters a diverse and unique set of pathogens, commensal microbes and other antigenic stimuli at the mucosal sites that potentially shape its microenvironment with regard to the development of innate defense mechanisms to protect against pathogens while counteracting pathogen–induced mucosal tissue damage (32-34). In the current study, we sought to compare the molecular and cellular profiles of host response during acute and chronic stages of SIV infection within the lung and GI mucosal compartments. We performed comparative analyses of viral replication, changes in T-cell subset distribution and function, and the profile of antiviral immune responses in the lung, jejunum, and colon. The IFN-α and the downstream signaling is important for controlling the viral dissemination during primary acute stages of infection. However, they are also associated with chronic immune activation/exhaustion in chronic viral diseases caused by HIV, LCMV, and Hepatitis C. Several important differences between the lung and GI mucosa with respect to IFN-α signaling, were identified prior to and during SIV infection that may potentially contribute to CD4+ T-cell restoration in the lung while resulting in incomplete CD4+ T-cell recovery in the jejunum and colon.

Maintenance of mucosal CD4+ T-cell subsets is critical for generating an effective immune response to pathogens (35-37). Effector memory T-cells (T_{EM}) are highly enriched at mucosal sites compared to peripheral blood or lymphoid tissues (29, 37). However, CCR5 expression on T_{EM} cells causes them to be highly susceptible targets for HIV and SIV infection (8, 38). While high numbers of memory CD4+ T-cells in the lung mucosa could prime this site for severe CD4+ T-cell depletion (39), we found that the highest levels of CD4+ T-cell depletion occurred in the jejunum and colon instead of the lung mucosa. These findings suggest that additional factors beyond the prevalence of effector memory CD4+ T-cells are likely to contribute to the divergent patterns of CD4+ T-cell depletion observed in each compartment. Moreover, the rapid rebound of CD4+ T-cells in BAL observed at two weeks post-SIV infection indicates that the lung mucosa has a greater capacity than the GI mucosa to restore and maintain resident helper CD4 T-cells following the duration of the primary SIV infection. Differences in the levels of MHCII+ APCs between lung and GI compartments could influence the magnitude of IFN-α expression. We determined that the level of macrophage infiltration in lung and GI mucosal compartments was similar. In addition, there was no significant difference in the expression levels of HLA-DR related transcripts (data not shown) in the lung and intestinal compartments. However, we cannot rule out a possibility that differential distribution of specific cell types such as pDC versus mDC populations within each compartment could still impact the level of type I interferon responses. This aspect warrants further investigation.

Our findings about the CD4+ T-cell rebound in BAL as well as preservation in the interstitial lung mucosa are in agreement with previous studies (29, 40). Collectively, they highlight a potential role of enhanced poly-functional CD8+ T-cell functionality in lung tissue during viral infection. We have previously shown that 50% or greater restoration of CD4+ T-cells in the gut mucosa of HIV infected patients receiving long-term HAART correlated with a marked increase in the polyfunctional antigen-specific CD8+ T-cells (41). Our findings in the SIV model provide further evidence, suggesting that better retention of

CD4+ T-cell numbers in the lung mucosa may increase the efficacy of type I IFN and SIV-specific CD8+ T-cell responses in that compartment compared to the GI mucosa. However, the rebound of CD4 T-cells in the lung may not be sustained in the absence of antiretroviral therapy since CD4+ T-cell depletion is observed during advanced stages of SIV infection as previously reported (29, 30). BAL samples contain the cells (including inflammatory cells) from distal airways and alveoli and represent lung luminal contents. Lung tissue samples consist of the cellular components of the lung parenchyma and represent T-cell populations present in the tissue microenvironment. Differences in the level of CD4+ T-cell rebound between BAL and lung tissues during SIV infection in our study suggest that changes in the T-cell subset distribution in the tissue environment may not be fully reflected in BAL.The T-cell subset data from BAL were obtained longitudinally during the initial 24 days of SIV infection, which showed CD4+ T-cell depletion during the primary acute stage of SIV infection that was followed by a rebound of the CD4+ T-cells. This is in agreement with previously reported findings showing depletion and rebound during acute infection (29). A significant proportion of CD4+ T-cells were preserved in the lung tissue. Importantly, our study demonstrates that the magnitude of CD4+ T-cell depletion in the lung tissue is lower compared to that in the gut tissue throughout infection with the exception of very early primary infection (<2 week). The CD4+ T-cell rebound in BAL and CD4+ T-cell preservation in lung tissue during early SIV infection correlated with a significant up-regulation of the expression of IFN-α responsive genes. During the chronic stages of SIV infection, the lung still retains more CD4+ T-cells as a percentage of total T-cells in comparison to both jejunum and colon mucosal compartments and this correlated with higher IFN-α expression in the lung. It is possible that the transition from primary acute stage into the chronic stages of viral infection, with higher CD4+ T-cell numbers in the lung compared to the gut, might provide an advantage of better functional host responses mediated through IFN-α signaling in the lung mucosa. Another possibility may include an increased tendency of the emergence of SIV variants during chronic or advanced SIV infection at one mucosal site compared to other that are resistant to the IFN-α defense response (42, 43). Importantly, previous studies have shown that BAL samples from HIV infected individuals had few memory CD4 T-cells with detectable provirus suggesting that there may be protective mechanisms in the lungs enabling CD4+ T-cell recovery (10, 29, 31). Moreover, IFN-α can also induce significant antiviral responses in dendritic cells that may limit the spread of HIV to CD4 T-cells from this cell population (44). Further studies are warranted to determine these host-viral interactions with respect to the kinetics of IFN-α responses and CD4+ T-cell depletion/rebound. Collectively, these findings suggest that therapeutic strategies designed to limit gut mucosal CD4+ T-cell depletion during primary acute stage of infection may provide substantial long-term benefits in establishing effective antiviral cellular and humoral responses.

The lung mucosa displayed the gene expression profile of a robust antiviral response compared to GI mucosal compartments. Despite similar viral loads in the lung and GI mucosa, an elevated expression of type I IFN associated viral restriction factors in the lung early during primary viral infection might have provided broader constraints over viral entry, replication, and budding. While we did not detect differences in viral burdens between compartments during the primary SIV infection, the CD4+ T-cell rebound/preservation

suggests that the immune response was protective to a certain extent. It is also possible that the viral load in the lung could have originated from infected monocytes trafficking into the lung microenvironment. These cells may have increased IFN-α expression and lead to prevention or inhibition of viral replication. Future investigation will help to identify the role of the cells harboring viral genomes at these mucosal sites in viral pathogenesis. Although type I IFNs stimulate the production of host viral restriction factors (45, 46), they also appear to play a pivotal role in the immunopathogenesis of HIV disease (47-49). Recent studies have shown that structural variants of IFN-α can ultimately promote different antiviral functions (50). In tandem, IFN-α can limit SIV replication in CD4 T-cells derived from AGMs suggesting that variants of IFN-α could have a positive association with better suppression of viral replication (13). In addition, supplementation with recombinant IFN-α strengthens the antiviral innate response and limits CD4 T-cell depletion in the rectum of Sooty mangabeys (51). It is not known whether IFN-α structural variants in the lung may contribute to greater antiviral benefit and reduced pathogenesis during SIV infection as compared to those in the GI mucosal compartments.

Greater retention and repopulation of helper CD4+ T-cells in the lung may also influence the quality of antiviral CD8+ T-cell responses in that compartment compared to those of the GI tract (10, 17, 22, 52, 53). While the mechanisms responsible for the differences in cytolytic CD8+ T-cell responses between the lung and intestinal mucosa remain to be explored, it is possible that diminished production of type I IFNs, chronic inflammation, and the depletion of CD4+ T-regulatory cells (54-56) could be contributing factors. In addition, non-cytolytic CD8+ T-cell responses in the lung may help to control SIV pathogenesis by preventing infection of incoming cells, while cytolytic responses may instead only control viral replication transiently during acute SIV infection (57, 58). Although the magnitude of CD8+ T-cell responses may not have been dramatically different between the lung and jejunum in our study, the quality of the anti-viral response (proliferation rates, perforin, and poly-functional cytokine production) in the lung may reflect the beneficial effects of the enhanced restoration and retention of CD4+ T-cells.

In summary, our findings provide novel insights into the molecular and cellular basis for differential mucosal immune responses in the lung and gastrointestinal mucosa during acute and chronic SIV infection. We present evidence that the lung employs a more robust type I interferon-driven response to SIV infection compared to the upper (jejunum) or lower (colon) gastrointestinal tract, and displays a better rebound in CD4+ T-cells during acute and chronic stages of infection. Progressive loss of CD4+ T cells is associated with progression to SAIDS (40). It is entirely possible that chronic IFN-α signaling in the lung may contribute to disease pathogenesis in the long-term. It is quite likely that factors other than IFN-α signaling could influence the level of CD4 T-cell rebound in the gut mucosa. Specifically, collagen disposition occurs rapidly in the intestinal tract and draining lymph nodes during SIV infection that could limit the restoration of the CD4+ T-cell population. However, this did not restrict CD8 T-cell infiltration suggesting that the impact of intestinal scarring and CD4+ T-cell repopulation warrants further investigation (59). A better understanding of the molecular mechanisms that drive the pulmonary response may identify valuable therapeutic targets that can be exploited to limit HIV pathogenesis. Vaccine and therapeutic strategies designed to stimulate effective innate responses early during primary

HIV infection in the intestinal mucosa may ultimately help to limit CD4+ T-cell depletion, dampen systemic viral dissemination, enhance antiviral CD8+ T-cell function in intestinal sites of chronic HIV replication despite HAART, and accelerate immune restoration in that compartment.

Acknowledgments

We thank Linda Hirst, Sona Santos and the animal care technicians at the California National Primate Research Center for their hard work and dedication.

This study was supported by grants from the National Institutes of Health (DK43183, AI43274, P51 RR000169). Dr. Sankaran was supported by NIH/BIRCWH K12 200911965.

References

1. Muller CA, Autenrieth IB, Peschel A. Innate defenses of the intestinal epithelial barrier. Cell Mol Life Sci. 2005; 62:1297–1307. [PubMed: 15971105]
2. Poonia B, Walter L, Dufour J, Harrison R, Marx PA, Veazey RS. Cyclic changes in the vaginal epithelium of normal rhesus macaques. J Endocrinol. 2006; 190:829–835. [PubMed: 17003283]
3. Brenchley JM,ST, Ruff LE, Price DA, Taylor JH, Beilman GJ, Nguyen PL, Khoruts A, Larson M, Haase AT, Douek DC. CD4+ T-cell depletion during all stages of HIV disease occurs predominantly in the gastrointestinal tract. Journal of Experimental Medicine. 2004; 200:749–759. [PubMed: 15365096]
4. George MD, Reay E, Sankaran S, Dandekar S. Early antiretroviral therapy for simian immunodeficiency virus infection leads to mucosal CD4+ T-cell restoration and enhanced gene expression regulating mucosal repair and regeneration. J Virol. 2005; 79:2709–2719. [PubMed: 15708990]
5. George MD, Sankaran S, Reay E, Gelli AC, Dandekar S. High-throughput gene expression profiling indicates dysregulation of intestinal cell cycle mediators and growth factors during primary simian immunodeficiency virus infection. Virology. 2003; 312:84–94. [PubMed: 12890623]
6. Guadalupe M, Reay E, Sankaran S, Prindiville T, Flamm J, McNeil A, Dandekar S. Severe CD4+ T-cell depletion in gut lymphoid tissue during primary human immunodeficiency virus type 1 infection and substantial delay in restoration following highly active antiretroviral therapy. J Virol. 2003; 77:11708–11717. [PubMed: 14557656]
7. Guadalupe M, Sankaran S, George MD, Reay E, Verhoeven D, Shacklett BL, Flamm J, Wegelin J, Prindiville T, Dandekar S. Viral suppression and immune restoration in the gastrointestinal mucosa of human immunodeficiency virus type 1-infected patients initiating therapy during primary or chronic infection. J Virol. 2006; 80:8236–8247. [PubMed: 16873279]
8. Mattapallil JJ, Douek DC, Hill B, Nishimura Y, Martin M, Roederer M. Massive infection and loss of memory CD4+ T-cells in multiple tissues during acute SIV infection. Nature. 2005; 434:1093–1097. [PubMed: 15793563]
9. Veazey RS, DeMaria M, Chalifoux LV, Shvetz DE, Pauley DR, Knight HL, Rosenzweig M, Johnson RP, Desrosiers RC, L. A.A. Gastrointestinal tract as a major site of CD4+ T-cell depletion and viral replication in SIV infection. Science. 1998; 280:427–431. [PubMed: 9545219]
10. Brenchley JM, Knox KS, Asher AI, Price DA, Kohli LM, Gostick E, Hill BJ, Hage CA, Brahmi Z, Khoruts A, Twigg HL 3rd, Schacker TW, Douek DC. High frequencies of polyfunctional HIV-specific T-cells are associated with preservation of mucosal CD4 T-cells in bronchoalveolar lavage. Mucosal Immunol. 2008; 1:49–58. [PubMed: 19079160]
11. Easlick J, Szubin R, Lantz S, Baumgarth N, Abel K. The early interferon alpha subtype response in infant macaques infected orally with SIV. J Acquir Immune Defic Syndr. 2010; 55:14–28. [PubMed: 20616742]
12. Alammar L, Gama L, Clements JE. Simian immunodeficiency virus infection in the brain and lung leads to differential type I IFN signaling during acute infection. J Immunol. 2011; 186:4008–4018. [PubMed: 21368232]

13. Bitzegeio J, Sampias M, Bieniasz PD, Hatziioannou T. Adaptation to the interferon-induced antiviral state by human and simian immunodeficiency viruses. J Virol. 2013; 87:3549–3560. [PubMed: 23325684]
14. Jacquelin B, Mayau V, Targat B, Liovat AS, Kunkel D, Petitjean G, Dillies MA, Roques P, Butor C, Silvestri G, Giavedoni LD, Lebon P, Barre-Sinoussi F, Benecke A, Muller-Trutwin MC. Nonpathogenic SIV infection of African green monkeys induces a strong but rapidly controlled type I IFN response. J Clin Invest. 2009; 119:3544–3555. [PubMed: 19959873]
15. Teijaro JR, Ng C, Lee AM, Sullivan BM, Sheehan KC, Welch M, Schreiber RD, de la Torre JC, Oldstone MB. Persistent LCMV infection is controlled by blockade of type I interferon signaling. Science. 2013; 340:207–211. [PubMed: 23580529]
16. Wilson EB, Yamada DH, Elsaesser H, Herskovitz J, Deng J, Cheng G, Aronow BJ, Karp CL, Brooks DG. Blockade of chronic type I interferon signaling to control persistent LCMV infection. Science. 2013; 340:202–207. [PubMed: 23580528]
17. Verhoeven D, Sankaran S, Silvey M, Dandekar S. Antiviral therapy during primary simian immunodeficiency virus infection fails to prevent acute loss of CD4+ T-cells in gut mucosa but enhances their rapid restoration through central memory T-cells. J Virol. 2008; 82:4016–4027. [PubMed: 18272585]
18. Leutenegger CM, Higgins J, Matthews TB, Tarantal AF, Luciw PA, Pedersen NC, N. T.W. Real-time TaqMan PCR as a specific and more sensitive alternative to the branched-chain DNA assay for quantitation of simian immunodeficiency virus RNA. AIDS Research and Human Retroviruses. 2001; 17:243–251. [PubMed: 11177407]
19. Hofmann-Lehmann R, Swenerton RK, Liska V, Leutenegger CM, Lutz H, McClure HM, Ruprecht RM. Sensitive and robust one-tube real-time reverse transcriptase-polymerase chain reaction to quantify SIV RNA load: comparison of one- versus two-enzyme systems. AIDS Res Hum Retroviruses. 2000; 16:1247–1257. [PubMed: 10957722]
20. Sankaran S, Guadalupe M, Reay E, George MD, Flamm J, Prindiville T, Dandekar S. Gut mucosal T-cell responses and gene expression correlate with protection against disease in long-term HIV-1-infected nonprogressors. Proc Natl Acad Sci U S A. 2005; 102:9860–9865. [PubMed: 15980151]
21. Clay CC, Rodrigues DS, Brignolo LL, Spinner A, Tarara RP, Plopper CG, Leutenegger CM, Esser U. Chemokine networks and in vivo T-lymphocyte trafficking in nonhuman primates. J Immunol Methods. 2004; 293:23–42. [PubMed: 15541274]
22. Ostrowski MA, Justement SJ, Ehler L, Mizell SB, Lui S, Mican J, Walker BD, Thomas EK, Seder R, Fauci AS. The role of CD4+ T-cell help and CD40 ligand in the in vitro expansion of HIV-1-specific memory cytotoxic CD8+ T-cell responses. J Immunol. 2000; 165:6133–6141. [PubMed: 11086046]
23. Holm GH, Gabuzda D. Distinct mechanisms of CD4+ and CD8+ T-cell activation and bystander apoptosis induced by human immunodeficiency virus type 1 virions. J Virol. 2005; 79:6299–6311. [PubMed: 15858014]
24. Richter R, Bistrian R, Escher S, Forssmann WG, Vakili J, Henschler R, Spodsberg N, Frimpong-Boateng A, Forssmann U. Quantum proteolytic activation of chemokine CCL15 by neutrophil granulocytes modulates mononuclear cell adhesiveness. J Immunol. 2005; 175:1599–1608. [PubMed: 16034099]
25. Pisabarro MT, Leung B, Kwong M, Corpuz R, Frantz GD, Chiang N, Vandlen R, Diehl LJ, Skelton N, Kim HS, Eaton D, Schmidt KN. Cutting edge: novel human dendritic cell- and monocyte-attracting chemokine-like protein identified by fold recognition methods. J Immunol. 2006; 176:2069–2073. [PubMed: 16455961]
26. Azzaoui I, Yahia SA, Chang Y, Vorng H, Morales O, Fan Y, Delhem N, Ple C, Tonnel AB, Wallaert B, Tsicopoulos A. CCL18 differentiates dendritic cells in tolerogenic cells able to prime regulatory T-cells in healthy subjects. Blood. 2011; 118:3549–3558. [PubMed: 21803856]
27. Barber SA, Gama L, Li M, Voelker T, Anderson JE, Zink MC, Tarwater PM, Carruth LM, Clements JE. Longitudinal analysis of simian immunodeficiency virus (SIV) replication in the lungs: compartmentalized regulation of SIV. J Infect Dis. 2006; 194:931–938. [PubMed: 16960781]

28. Lewin SR, Kirihara J, Sonza S, Irving L, Mills J, Crowe SM. HIV-1 DNA and mRNA concentrations are similar in peripheral blood monocytes and alveolar macrophages in HIV-1-infected individuals. AIDS. 1998; 12:719–727. [PubMed: 9619803]

29. Okoye A, Meier-Schellersheim M, Brenchley JM, Hagen SI, Walker JM, Rohankhedkar M, Lum R, Edgar JB, Planer SL, Legasse A, Sylwester AW, Piatak M Jr. Lifson JD, Maino VC, Sodora DL, Douek DC, Axthelm MK, Grossman Z, Picker LJ. Progressive CD4+ central memory T-cell decline results in CD4+ effector memory insufficiency and overt disease in chronic SIV infection. J Exp Med. 2007; 204:2171–2185. [PubMed: 17724130]

30. Sopper S, Nierwetberg D, Halbach A, Sauer U, Scheller C, Stahl-Hennig C, Matz-Rensing K, Schafer F, Schneider T, ter Meulen V, Muller JG. Impact of simian immunodeficiency virus (SIV) infection on lymphocyte numbers and T-cell turnover in different organs of rhesus monkeys. Blood. 2003; 101:1213–1219. [PubMed: 12393472]

31. Knox KS, Vinton C, Hage CA, Kohli LM, Twigg HL 3rd, Klatt NR, Zwickl B, Waltz J, Goldman M, Douek DC, Brenchley JM. Reconstitution of CD4 T-cells in bronchoalveolar lavage fluid after initiation of highly active antiretroviral therapy. J Virol. 2010; 84:9010–9018. [PubMed: 20610726]

32. Brenchley JM, Price DA, Douek DC. HIV disease: fallout from a mucosal catastrophe? Nat Immunol. 2006; 7:235–239. [PubMed: 16482171]

33. Iwasaki A. Mucosal dendritic cells. Annu Rev Immunol. 2007; 25:381–418. [PubMed: 17378762]

34. Sansonetti PJ. War and peace at mucosal surfaces. Nat Rev Immunol. 2004; 4:953–964. [PubMed: 15573130]

35. Lanzavecchia A, Sallusto F. Dynamics of T lymphocyte responses: intermediates, effectors, and memory cells. Science. 2000; 290:92–97. [PubMed: 11021806]

36. Lanzavecchia A, Sallusto F. Understanding the generation and function of memory T-cell subsets. Curr Opin Immunol. 2005; 17:326–332. [PubMed: 15886125]

37. Sallusto F, Geginat J, Lanzavecchia A. Central memory and effector memory T-cell subsets: function, generation, and maintenance. Annu Rev Immunol. 2004; 22:745–763. [PubMed: 15032595]

38. Picker LJ, Reed-Inderbitzin EF, Hagen SI, Edgar JB, Hansen SG, Legasse A, Planer S, Piatak M Jr. Lifson JD, Maino VC, Axthelm MK, Villinger F. IL-15 induces CD4 effector memory T-cell production and tissue emigration in nonhuman primates. J Clin Invest. 2006; 116:1514–1524. [PubMed: 16691294]

39. Hansen SG, Vieville C, Whizin N, Coyne-Johnson L, Siess DC, Drummond DD, Legasse AW, Axthelm MK, Oswald K, Trubey CM, Piatak M Jr. Lifson JD, Nelson JA, Jarvis MA, Picker LJ. Effector memory T-cell responses are associated with protection of rhesus monkeys from mucosal simian immunodeficiency virus challenge. Nat Med. 2009; 15:293–299. [PubMed: 19219024]

40. Picker LJ, Hagen SI, Lum R, Reed-Inderbitzin EF, Daly LM, Sylwester AW, Walker JM, Siess DC, Piatak M Jr. Wang C, Allison DB, Maino VC, Lifson JD, Kodama T, Axthelm MK. Insufficient production and tissue delivery of CD4+ memory T-cells in rapidly progressive simian immunodeficiency virus infection. J Exp Med. 2004; 200:1299–1314. [PubMed: 15545355]

41. Macal M, Sankaran S, Chun TW, Reay E, Flamm J, Prindiville TJ, Dandekar S. Effective CD4+ T-cell restoration in gut-associated lymphoid tissue of HIV-infected patients is associated with enhanced Th17 cells and polyfunctional HIV-specific T-cell responses. Mucosal Immunol. 2008; 1:475–488. [PubMed: 19079215]

42. Humes D, Overbaugh J. Adaptation of subtype a human immunodeficiency virus type 1 envelope to pigtailed macaque cells. J Virol. 2011; 85:4409–4420. [PubMed: 21325401]

43. Thippeshappa R, Ruan H, Wang W, Zhou P, Kimata JT. A variant macaque-tropic human immunodeficiency virus type 1 is resistant to alpha interferon-induced restriction in pig-tailed macaque CD4+ T-cells. J Virol. 2013; 87:6678–6692. [PubMed: 23552412]

44. Mohanram V, Skold AE, Bachle SM, Pathak SK, Spetz AL. IFN-alpha induces APOBEC3G, F, and A in immature dendritic cells and limits HIV-1 spread to CD4+ T-cells. J Immunol. 2013; 190:3346–3353. [PubMed: 23427247]

45. Pillai SK, Abdel-Mohsen M, Guatelli J, Skasko M, Monto A, Fujimoto K, Yukl S, Greene WC, Kovari H, Rauch A, Fellay J, Battegay M, Hirschel B, Witteck A, Bernasconi E, Ledergerber B,

Gunthard HF, Wong JK, Swiss HIVCS. Role of retroviral restriction factors in the interferon-alpha-mediated suppression of HIV-1 in vivo. Proc Natl Acad Sci U S A. 2012; 109:3035–3040. [PubMed: 22315404]

46. Goldstone DC, Ennis-Adeniran V, Hedden JJ, Groom HC, Rice GI, Christodoulou E, Walker PA, Kelly G, Haire LF, Yap MW, de Carvalho LP, Stoye JP, Crow YJ, Taylor IA, Webb M. HIV-1 restriction factor SAMHD1 is a deoxynucleoside triphosphate triphosphohydrolase. Nature. 2011; 480:379–382. [PubMed: 22056990]
47. Boasso A, Royle CM, Doumazos S, Aquino VN, Biasin M, Piacentini L, Tavano B, Fuchs D, Mazzotta F, Lo Caputo S, Shearer GM, Clerici M, Graham DR. Overactivation of plasmacytoid dendritic cells inhibits antiviral T-cell responses: a model for HIV immunopathogenesis. Blood. 2011; 118:5152–5162. [PubMed: 21931112]
48. Herbeuval JP, Shearer GM. HIV-1 immunopathogenesis: how good interferon turns bad. Clin Immunol. 2007; 123:121–128. [PubMed: 17112786]
49. Chang JJ, Altfeld M. Innate immune activation in primary HIV-1 infection. J Infect Dis 202 Suppl. 2010; 2:S297–301.
50. Vazquez N, Schmeisser H, Dolan MA, Bekisz J, Zoon KC, Wahl SM. Structural variants of IFNalpha preferentially promote antiviral functions. Blood. 2011; 118:2567–2577. [PubMed: 21757613]
51. Vanderford TH, Slichter C, Rogers KA, Lawson BO, Obaede R, Else J, Villinger F, Bosinger SE, Silvestri G. Treatment of SIV-infected sooty mangabeys with a type-I IFN agonist results in decreased virus replication without inducing hyperimmune activation. Blood. 2012; 119:5750–5757. [PubMed: 22550346]
52. Kalams SA, Walker BD. The critical need for CD4 help in maintaining effective cytotoxic T lymphocyte responses. J Exp Med. 1998; 188:2199–2204. [PubMed: 9858506]
53. Sumpter B, Dunham R, Gordon S, Engram J, Hennessy M, Kinter A, Paiardini M, Cervasi B, Klatt N, McClure H, Milush JM, Staprans S, Sodora DL, Silvestri G. Correlates of preserved CD4(+) T-cell homeostasis during natural, nonpathogenic simian immunodeficiency virus infection of sooty mangabeys: implications for AIDS pathogenesis. J Immunol. 2007; 178:1680–1691. [PubMed: 17237418]
54. Chase AJ, Yang HC, Zhang H, Blankson JN, Siliciano RF. Preservation of FoxP3+ regulatory T-cells in the peripheral blood of human immunodeficiency virus type 1-infected elite suppressors correlates with low CD4+ T-cell activation. J Virol. 2008; 82:8307–8315. [PubMed: 18579608]
55. Barnes MJ, Powrie F. Regulatory T-cells reinforce intestinal homeostasis. Immunity. 2009; 31:401–411. [PubMed: 19766083]
56. Manion M, Rodriguez B, Medvik K, Hardy G, Harding CV, Schooley RT, Pollard R, Asmuth D, Murphy R, Barker E, Brady KE, Landay A, Funderburg N, Sieg SF, Lederman MM. Interferon-alpha administration enhances CD8+ T-cell activation in HIV infection. PLoS One. 2012; 7:e30306. [PubMed: 22291932]
57. Klatt NR, Shudo E, Ortiz AM, Engram JC, Paiardini M, Lawson B, Miller MD, Else J, Pandrea I, Estes JD, Apetrei C, Schmitz JE, Ribeiro RM, Perelson AS, Silvestri G. CD8+ lymphocytes control viral replication in SIVmac239-infected rhesus macaques without decreasing the lifespan of productively infected cells. PLoS Pathog. 2010; 6:e1000747. [PubMed: 20126441]
58. Wong JK, Strain MC, Porrata R, Reay E, Sankaran-Walters S, Ignacio CC, Russell T, Pillai SK, Looney DJ, Dandekar S. In vivo CD8+ T-cell suppression of siv viremia is not mediated by CTL clearance of productively infected cells. PLoS Pathog. 2010; 6:e1000748. [PubMed: 20126442]
59. Estes J, Baker JV, Brenchley JM, Khoruts A, Barthold JL, Bantle A, Reilly CS, Beilman GJ, George ME, Douek DC, Haase AT, Schacker TW. Collagen deposition limits immune reconstitution in the gut. J Infect Dis. 2008; 198:456–464. [PubMed: 18598193]

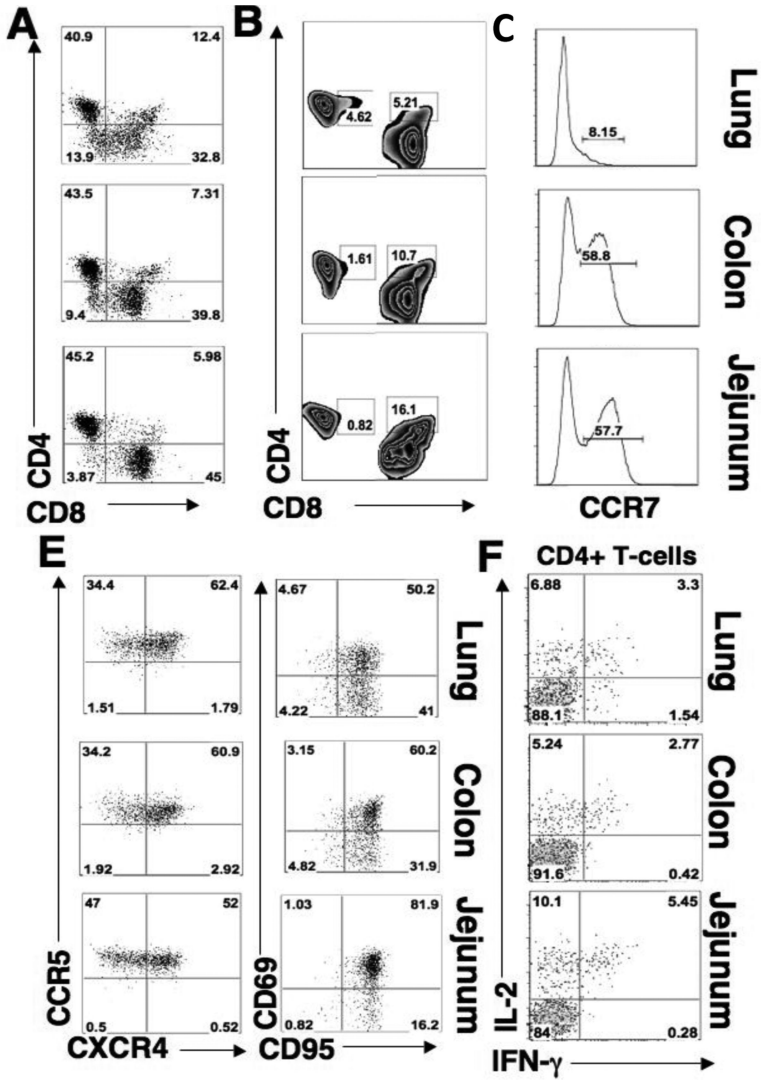

Figure 1. Lung and gastrointestinal mucosal sites have comparable levels of activated memory CD4+ T-cells

Flow cytometry was performed to determine the percentages of CD4+ and CD8+ T-cells in uninfected mucosal tissues with respect to lymphocyte subtypes. **(A)** Percentage of CD4+ versus CD8+ in lung (upper), colon (middle), and jejunum (lower). **(B)** Percentage of CD4+ T-cells that co-express CD8 (CD4+highCD8+low) and the percentage of CD8+ T-cells that express CD4+ (CD8+highCD4+low) in mucosa. **(C)** Percentage of central memory (CCR7+) CD4+ T-cells in lung, colon, and jejunum. **(D)** Percentage of CD4+ T-cells that express CCR5 or CXCR4 in lung, colon, and jejunum. **(E)** Percentage of CD4+ T-cells that express CD95 versus CD69 in lung, colon, and jejunum. **(F)** Percentage of CD4+ T-cells cells that secrete IL-2 or IFN-γ upon SEB stimulation.

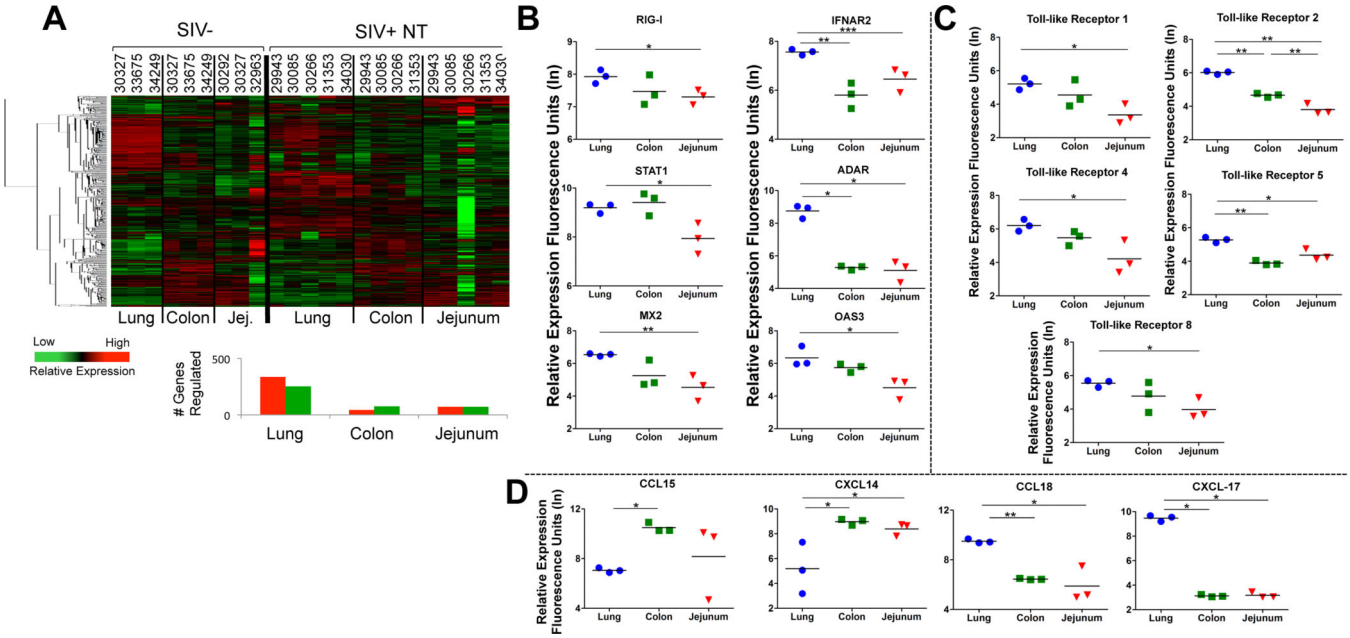

Figure 2. Distinct profiles of immune response associated gene expression in the lung and GI mucosa of therapy-naïve SIV infected animals and healthy controls

(A) Hierarchical clustering of the genes with increased or decreased expression in the lung, colon, and jejunum of untreated SIV infected animals. (SIV+ NT indicates SIV+ animals without therapy). Baseline levels of transcription of genes associated with **(B)** type I IFN response (RIG-I, IFNAR2, STAT-1, ADAR, MX2, OAS3), **(C)** pathogen associated molecular patterns, or PAMPS (TLR1, 2, 4, 5, and 8); and **(D)** trafficking (CCL15, CXCL14, CCL18, CXCL17) are shown in the lung (blue circles), colon (green squares), and jejunum (red triangles) tissues of healthy macaques (n=3) were determined by microarray analysis. *p-value<0.05, **p-value<0.01, ***p-value<0.001

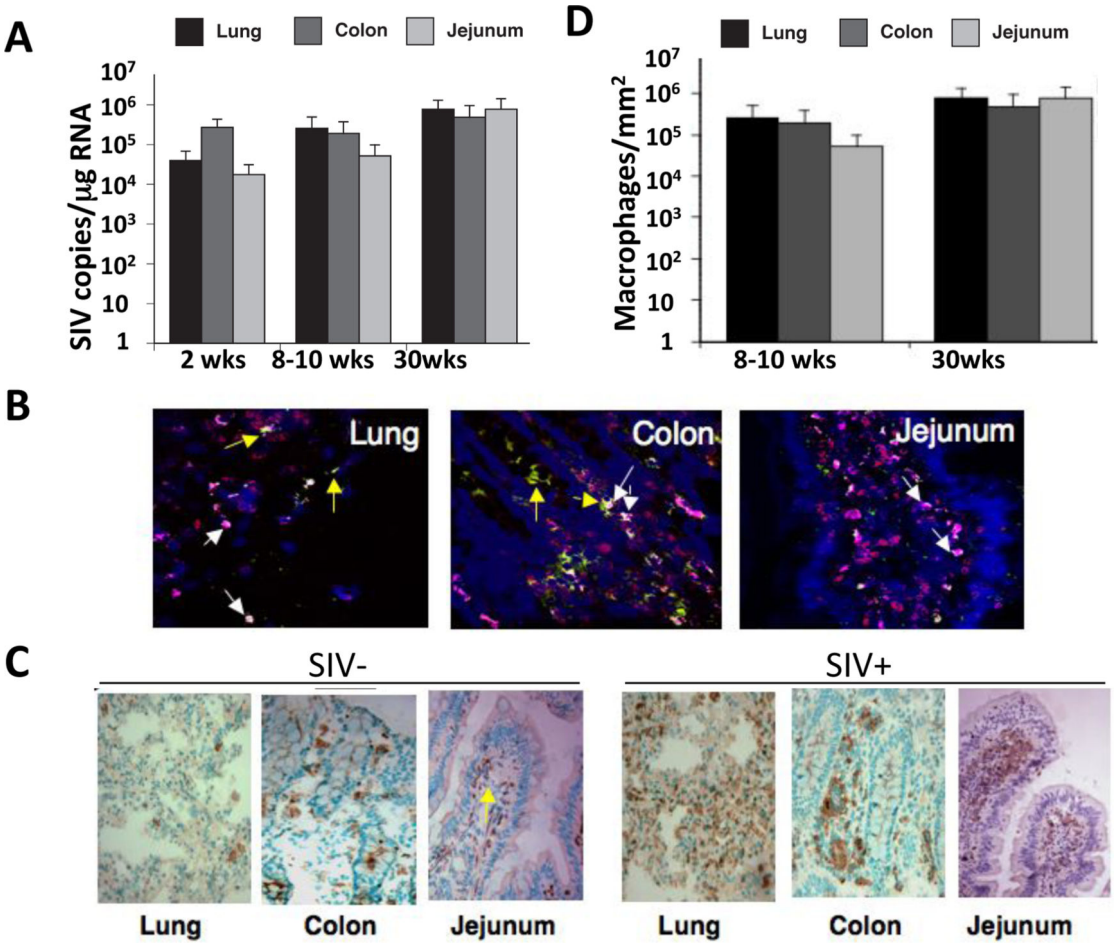

Figure 3. Comparable levels of SIV replication in the lung and gastrointestinal mucosal compartments

(A) Comparison of mucosal viral loads (determined by real-time PCR) in the lung (black bars), colon (light gray), and jejunum (dark gray) at 8-10 weeks post infection (p.i.), and again at 30 weeks p.i. SIV copy numbers in each tissue were calculated with respect to a standard curve generated by samples with known copy numbers and values represent averages across 5 animals in each group. (mean, +/− standard error). **(B)** Detection and identification of SIV-infected cells was performed by immunohistochemical analysis. Location of the cells expressing SIV p27 (red color) was mapped in each 25 mucosal compartment at 30 weeks p.i. Tissues were co-stained for CD3 (green color) and Ham56 (magenta color) to determine if SIV infected cells were T-cells or macrophages, respectively. Yellow arrows represent infected CD4+ T-cells while white arrows represent infected macrophages **(C)** Immunohistochemical assessment of Ham56 expression indicated a similar influx of macrophages into mucosal compartments 30 weeks p.i. **(D)** Quantitation of Ham56+ cells in the lung, colon, and jejunum at 30 weeks post-infection (mean +/− standard error, n=3).

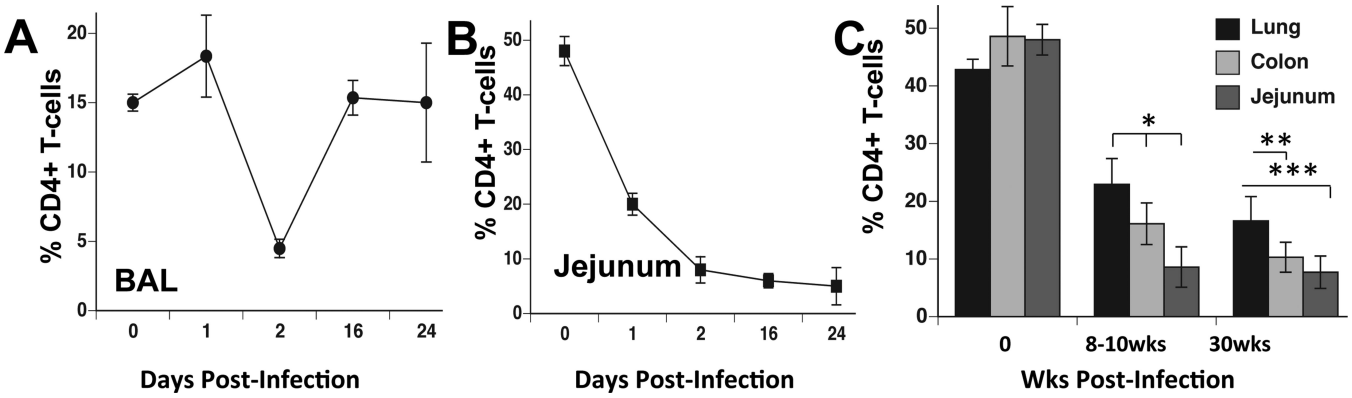

Figure 4. Early CD4+ T-cell rebound in the lung mucosa while sustained CD4+ T-cell depletion in the gut mucosal sites during SIV infection

Flow cytometric analysis was performed for longitudinal assessment of CD4+ T-cell percentages from **(A)** BAL or **(B)** jejunum during early (first 24 days) and primary SIV infection (n=4 BAL, n=5 for jejunum, +/− standard error). (**C)** Flow cytometric analysis was performed to determine percentages of memory CD4+ T-cells (of total CD3+ T-cells) retained in the lung (total lung tissue), colon, and jejunum of macaques at 8-10 weeks post-infection and at 30 weeks post-infection (mean, +/− standard error, n=5).

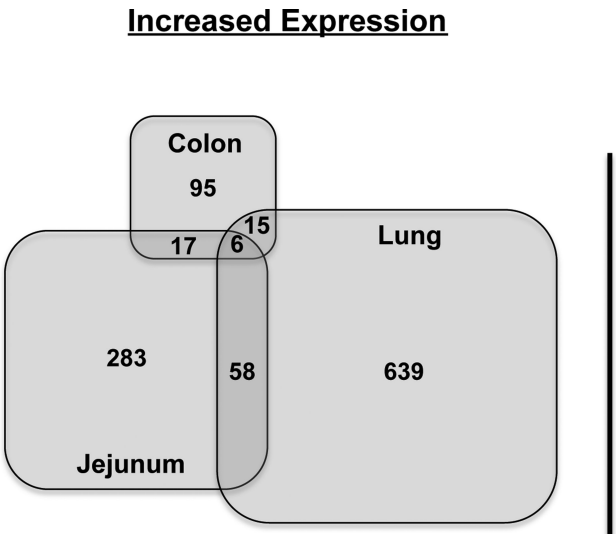

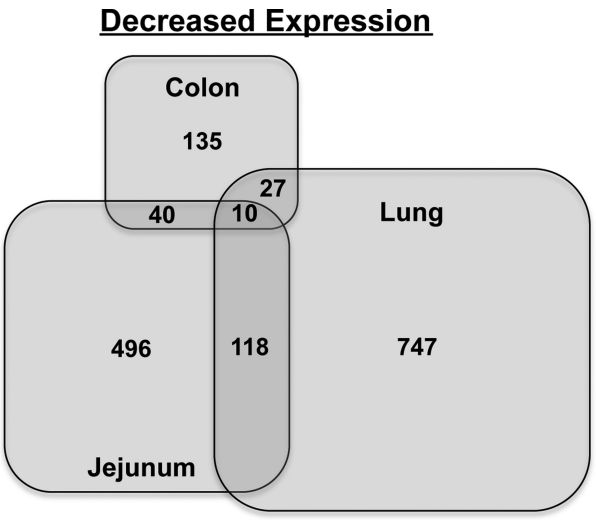

	Pathway/Process	# Genes	%	*p* value
Lung	Mitosis	37	5.25	5.6×10^{-23}
	Apoptosis	60	8.51	9.3×10^{-9}
	Response to virus	18	2.55	9.6×10^{-8}
	Anti-apoptosis	19	2.70	4.6×10^{-5}
	Adaptive immune response	8	1.13	2.7×10^{-2}
Jejunum	UBL conjugation	19	5.40	2.0×10^{-4}
	DNA packaging	15	4.26	3.0×10^{-3}
	Acetylation	20	5.68	9.8×10^{-3}
	Response to virus	6	1.70	3.8×10^{-2}
	Anti-apoptosis	8	2.27	4.0×10^{-2}
Colon	Response to chemical stimulus	11	8.53	7.4×10^{-3}
	Cell adhesion	12	9.30	1.5×10^{-2}
	Stress response	14	10.85	2.8×10^{-2}
	UBL conjugation	7	5.43	3.3×10^{-5}
	Signal transduction	34	26.36	4.9×10^{-2}

	Pathway/Process	# Genes	%	*p* value
Lung	Insulin receptor signaling	12	1.35	2.7×10^{-7}
	Apoptosis	65	7.30	1.8×10^{-6}
	Growth factor binding	13	1.46	7.5×10^{-5}
	Cell cycle regulation	41	4.61	7.7×10^{-4}
	AKT signaling	7	0.79	1.5×10^{-3}
Jejunum	Inflammatory response	43	6.55	3.8×10^{-15}
	Defense response	54	8.23	2.8×10^{-11}
	Extracellular region	83	12.65	6.9×10^{-7}
	Wound healing	18	2.74	1.5×10^{-6}
	Chemotaxis	18	2.74	1.1×10^{-5}
Colon	Apoptosis	18	8.65	1.6×10^{-3}
	Cell proliferation	18	8.65	1.8×10^{-3}
	Oxidoreductase activity	18	8.65	9.5×10^{-3}
	EGF receptor signaling	3	1.44	3.6×10^{-2}
	Extracellular region	11	5.29	4.9×10^{-2}

Figure 5. Divergent molecular profiles of immune response to SIV infection in the lung and intestinal mucosa

Alterations in mucosal gene expression were determined by microarray analysis of lung, colon, and jejunum samples from chronically SIV infected animals (n=5) versus healthy uninfected controls (n=5). Venn diagrams reflect the different numbers (size) of up and down regulated genes in the lung, colon, and jejunum, as well as the overlaps in regulation between compartments. The predominant biological pathways and processes statistically (p-value < 0.05) implicated by the genes modulated at each mucosal site during SIV infection are shown in the bottom panel.

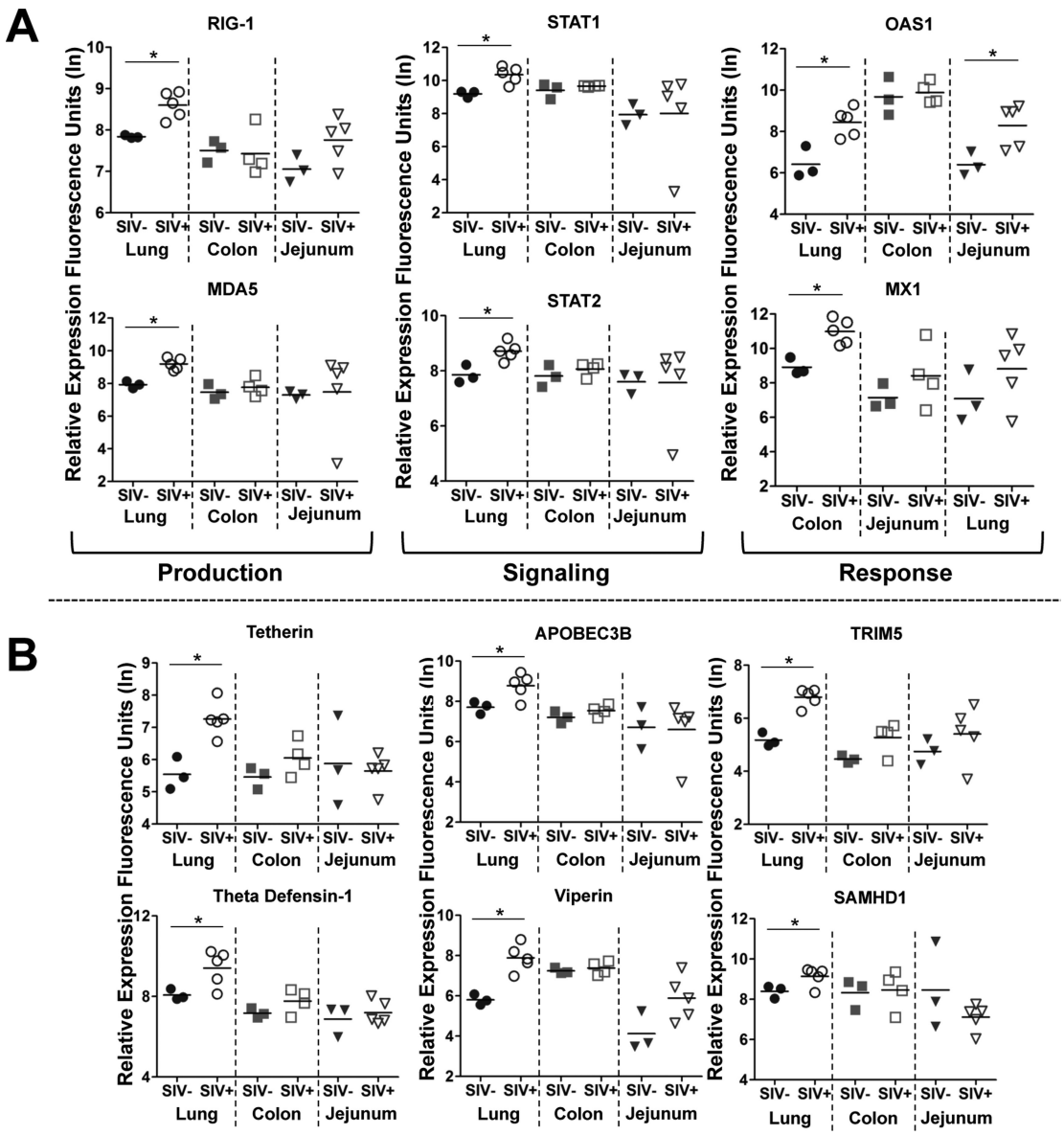

Figure 6. Distinct innate anti-viral gene expression in the lung compared to gastrointestinal mucosa during chronic SIV infection

(A) Changes in the expression of molecules associated with type I interferon (IFN) production (RIG-I, MDA-5), signaling (STAT1, STAT2) and response (OAS1, MX1) between healthy and chronically SIV infected animals was determined in the lung, colon and jejunum by DNA microarray analysis. **(B)** Comparison of the induction of type I IFN-stimulated retroviral restriction 26 factors, BST2/tetherin APOBEC3B, TRIM5, theta defensin-1, SAMHDI, and viperin in the lung, colon, and jejunum during chronic SIV infection. *p-value<0.05

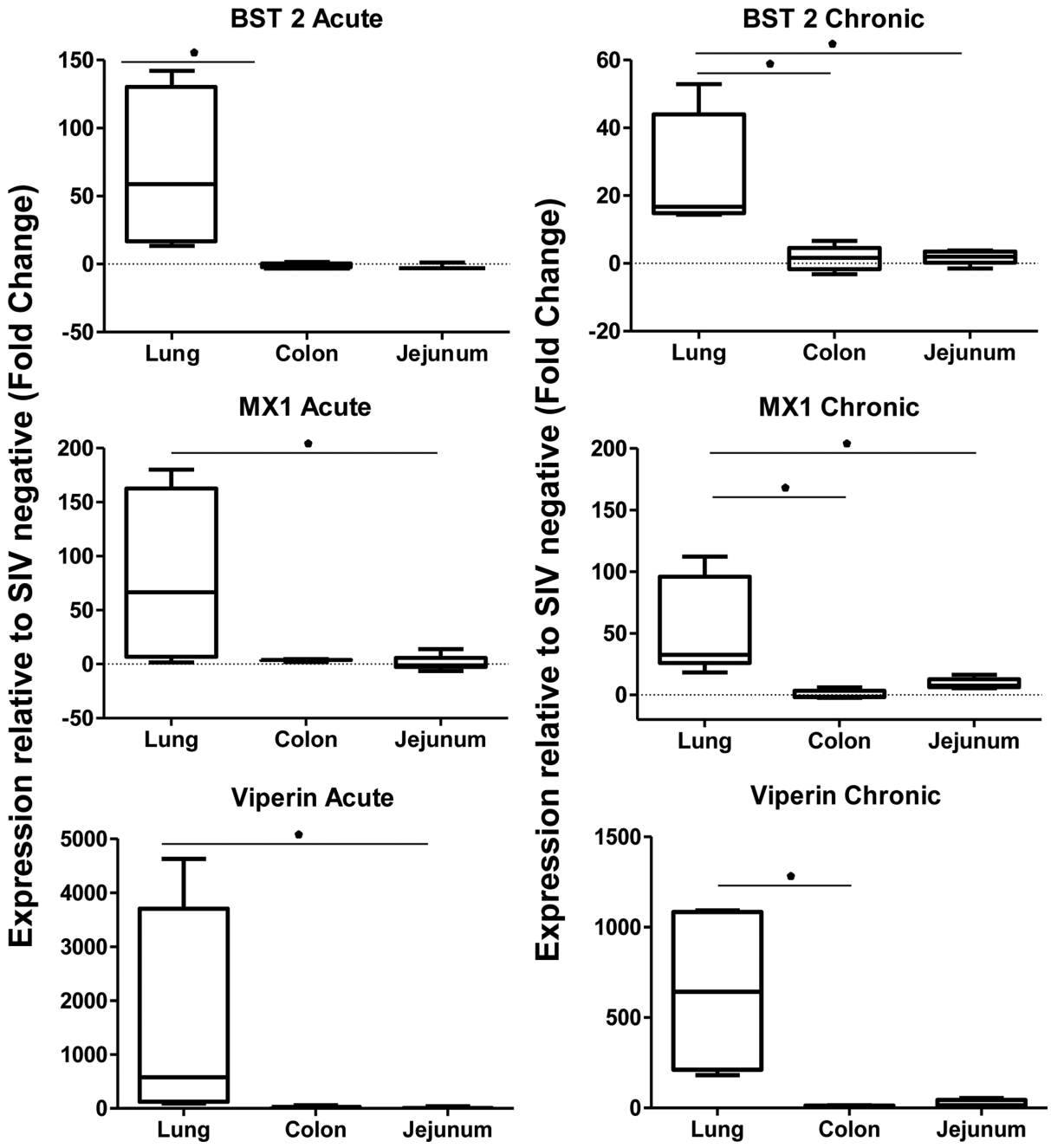

Figure 7. Divergent induction of viral restriction factors in the lung and GI tract initiates during early stage SIV infection

Induction of BST2/tetherin, MX-1, and Viperin was measured by quantitative RT-PCR in the lungs, colon and jejunum during the acute (2 wks post infection) and chronic stages of SIV infection (30 wks post infection). Results are presented as fold-changes with respect to uninfected controls. *p-value<0.05

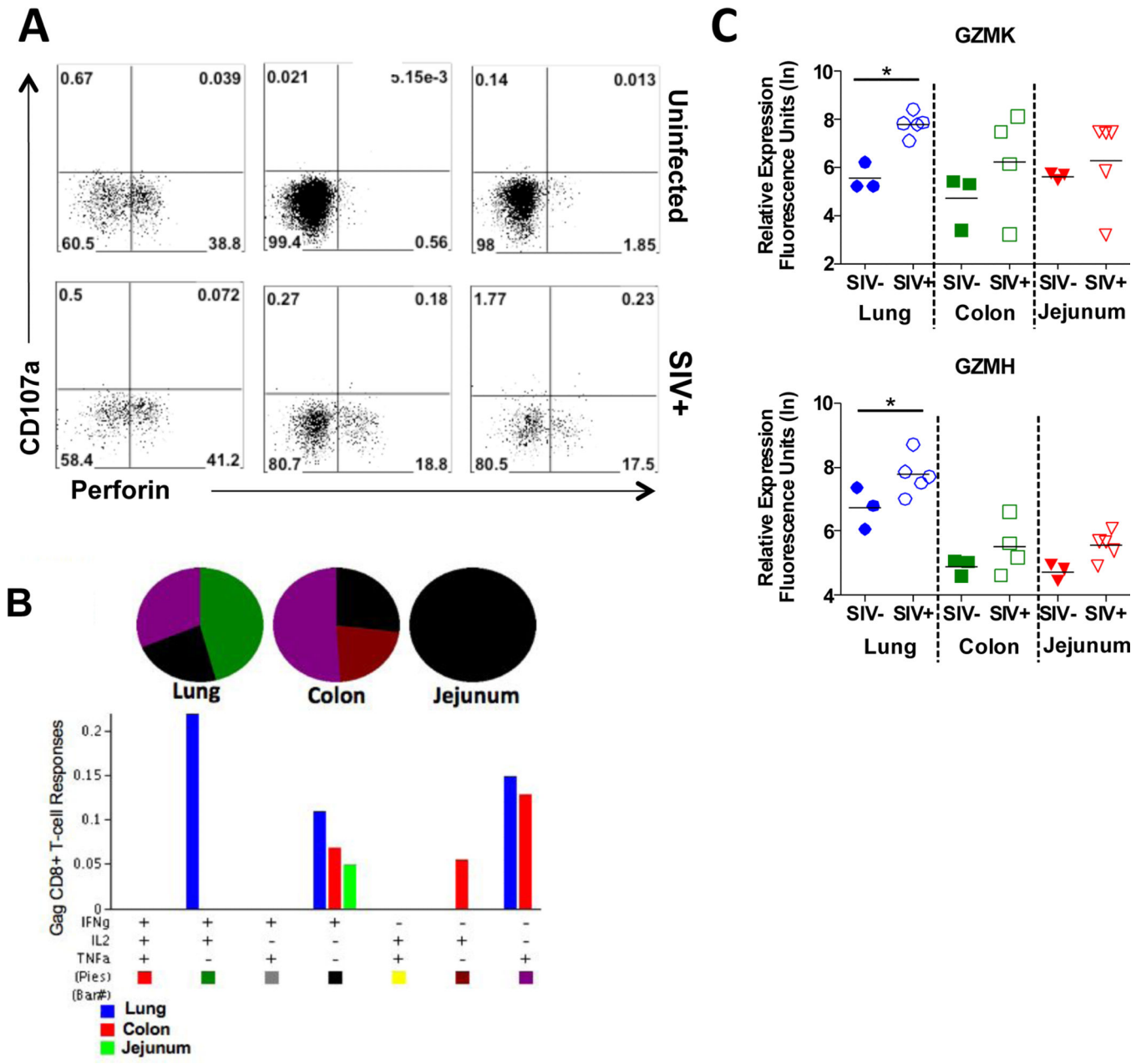

Figure 8. Comparison of lung and GI tract CD8+ T-cell responses in SIV infected macaques

(A) Flow cytometric analysis of changes in CD8+ T-cell populations in the lung, colon, and jejunum expressing perforin and/or the degranulation marker, CD107a in response to SIV infection. A representative animal shown, (n=5). **(B)** *In vitro* production of IFNγ, IL-2, and TNFα in response to SIV gag stimulation was evaluated in CD8+ T-cells isolated from the lung, colon, and jejunum at 10 weeks post SIV infection (n=5). **(C)** Changes in the expression of granzymes K and H in the lung, colon, and jejunum during chronic stage SIV infection were determined by microarray analysis. *p-value<0.05